Global patterns and drivers of soil total phosphorus concentration

Xianjin He[1, 2]; Laurent Augusto[3]; Daniel S. Goll[4]; Bruno Ringeval[3]; Yingping Wang[5]; Julian Helfenstein[6]; Yuanyuan Huang[4,5]; Kailiang Yu[7]; Zhiqiang Wang[8]; Yongchuan Yang[1]; Enqing Hou[2]

1 Key Laboratory of the Three Gorges Reservoir Region's Eco-Environment, Ministry of Education, Chongqing University, Chongqing, 400045, China

2 Key Laboratory of Vegetation Restoration and Management of Degraded Ecosystems, South China Botanical Garden, Chinese Academy of Sciences, Guangzhou, China

3 INRAE, Bordeaux Sciences Agro, UMR 1391 ISPA, 33140 Villenave d'Ornon, France

4 Université Paris Saclay, CEA-CNRS-UVSQ, LSCE/IPSL, Gif sur Yvette, France

5 CSIRO Oceans and Atmosphere, Aspendale, Vic., Australia

6 Agroscope, 8046 Zürich, Switzerland

7 High Meadows Environmental Institute, Princeton University, Princeton, NJ 08544, USA

8 Institute for Advanced Study, Chengdu University, Chengdu, Sichuan, China

Corresponding to: Yongchuan Yang (ycyang@cqu.edu.cn); Enqing Hou (houeq@scbg.ac.cn).

Abstract. Soil represents the largest phosphorus (P) stock in terrestrial ecosystems. Determines the amount of soil P is a critical first step for identifying sites where ecosystem functioning is potentially limited by soil P availability. However, global patterns and predictors of soil total P concentration remain poorly understood. To address this knowledge gap, we constructed a database of total P concentration of 5,275 globally distributed (semi-)natural soils from 761 published studies. We quantified the relative importance of 13 soil-forming variables in predicting soil total P concentration and then made further predictions at the global scale using a random forest approach. Soil total P concentration varied significantly among parent material types, soil orders, biomes, and continents, and ranged widely from 1.4 to 9,630.0 (median 430.0 and mean 570.0) mg kg^{-1} across the globe. About two-thirds (65%) of the global variation was accounted for by the 13 variables that we selected, among which soil organic carbon concentration, parent material, mean annual temperature, and soil sand content were the most important ones. While predicted soil total P concentrations increased significantly with latitude, they varied largely among regions with similar latitudes due to regional differences in parent material, topography, and/or climate conditions. Soil P stocks (excluding Antarctica) were estimated to be 26.8 ± 3.1 (mean ± standard deviation) Pg and 62.2 ± 8.9 Pg (1 Pg=1×10^{15} g) in the topsoil (0-30 cm) and subsoil (30-100 cm), respectively. Our global map of soil total P concentration as well as the underlying drivers of soil total P concentration can be used to constraint Earth system models that represent the P cycle and to inform quantification of global soil P availability. Raw datasets and global maps generated in this study are available at https://doi.org/10.6084/m9.figshare.14583375 (He et al., 2021).

1 Introduction

In terrestrial ecosystems, to a depth of one meter from the land surface, most of the P is found in the soil (Zhang et

33 al., 2021). The amount and form of P determine the supply of soil P to plants, which further regulate the structure and function

34 of global terrestrial ecosystems (Vitousek et al., 2010; Hou et al., 2020; Elser et al., 2007; Hou et al., 2021). Moreover, the

35 amount or total concentration of P in soils determines P concentration in all major forms in soils (Hou et al., 2018a;

36 Turner and Engelbrecht, 2011). Therefore, it is important to determine the total concentration of P in soils, which varies up

37 to three orders of magnitude across the globe (Yanai, 1998; Augusto et al., 2010; Zhang et al., 2021). Despite the large variation

38 in soil total P concentration, its global patterns and drivers remain poorly resolved and improving this knowledge gap is needed

39 to better represent the P cycle in Earth system models (Fleischer et al., 2019; Goll et al., 2017; Reed et al., 2015; Wang et al.,

40 2015; Wieder et al., 2015; Zhang et al., 2011; Achat et al., 2016a).

41   Soil total P concentration is the outcome of climatic, biotic, and landscape processes interacting over time on soil parent

42 material (Dokuchaev, 1883; Jenny, 1941; Buendía et al., 2010). Each of these factors may be characterized by a few variables;

43 for example, climate may be characterized by mean annual temperature (MAT) and precipitation (MAP). Relationships

44 between soil total P concentration and variables such as parent material type and P concentration, MAT, MAP, site slope, and

45 soil organic carbon (SOC) have been reported in previous studies, but mostly at local to regional scales (Brédoire et al., 2016;

46 Cheng et al., 2018; Li et al., 2019; Porder and Chadwick, 2009; Wang et al., 2009). Few studies have quantified the relative

47 importance of these variables for predicting soil total P concentration at a global scale (Delgado-Baquerizo et al., 2020;

48 Augusto et al., 2017; Yang et al., 2013). Such an understanding can guide the management of the soil P supply in

49 agroecosystems of different regions (Ringeval et al., 2017) and is crucial for both mapping soil total P concentration in natural

50 terrestrial ecosystems (Reed et al., 2015) and simulating ecosystem functioning (Achat et al., 2016a).

51   While each soil-forming factor can determine soil total P concentration, the roles of some factors (e.g., climate and

52 vegetation) are less understood than other factors (e.g., parent material and soil age). Since P in soil is derived mainly from

53 parent materials, the control of parent material on soil total P concentration has been well recognized (Augusto et al., 2017;

54 Porder and Ramachandran, 2013). Soil chronosequences provide a unique opportunity to isolate the effect of soil age from

55 other soil-forming factors on soil P dynamics, and have shown that soil age negatively impacts soil total P concentration

56 (Wardle et al., 2004; Delgado-Baquerizo et al., 2020; Vitousek et al., 2010; Walker and Syers, 1976). Due to climate change,

57 there is an increasing interest in how climate impacts soil total P concentration (Augusto et al., 2017; Vitousek and Chadwick,

58 2013; Hou et al., 2018a). Yet the effects of climate, vegetation, and topography on soil total P concentration remain largely

59 unknown. Recently, Delgado-Baquerizo et al. (2020) surveyed 32 ecosystem properties, including soil total P concentration,

60 in 16 soil chronosequences globally. They found that climate, vegetation, topography, and soil age together explained only

61 about 60% of the variation in soil total P concentration, despite examining 30 predictors and considering all possible

62 interactions among predictors. This finding reflects our incomplete understanding of the controls of soil total P concentration.

63   Several pressing global issues such as mitigating climate change, increasing food security, and reducing nutrient run-off to

64 bodies of water, rely on accurate soil P maps (Alewell et al., 2020; Ringeval et al., 2017; Beusen et al., 2015; Wang et al.,

65 2010). While several maps of soil total P concentration have been produced (Viscarra Rossel and Bui, 2016; Ballabio et al.,

66 2019; Hengl et al., 2017a; Delmas et al., 2015), to our knowledge, there are only two published maps of soil total P

67 concentration in natural terrestrial ecosystems (Shangguan et al., 2014; Yang et al., 2013). These two maps have been used to

68 explore global patterns of soil P supply (Yang et al., 2013), estimate P limitation on future terrestrial C sequestration (Sun et

69 al., 2017), and used as baseline information to quantify P supply in agricultural ecosystems (Ringeval et al., 2017). They are

70 also used frequently in land surface models to benchmark soil P modules (Yang et al., 2014; Goll et al., 2012). However, the

71 two maps may suffer from large uncertainties due to limited numbers of predictors used and/or low spatial coverage of global

72 soils. First, for example, Yang et al. (2013) mapped soil total P concentration based only on parent material and soil

73 chronosequence measurements. The map by Shangguang et al. (2014) was based on a database that had poor coverage of many

74 parts of the world (e.g. high latitude, Africa, South America). Second, both maps only focus on the surface layers of soils,

75 though subsoils are known to contribute to the P nutrition of plants and P leaching to groundwater (Rodionov et al., 2020;

76 Andersson et al., 2013).

77   To address these issues, we constructed a global database of total P concentration of 5,275 (semi-)natural soils from 761

78 published studies. We defined (semi-)natural ecosystems as ecosystems without any documented significant anthropogenic

79 activities such as tillage, fertilization, and heavy grazing. We then used random forest algorithms to quantify the relative

80 importance of soil-forming variables for predicting soil total P concentration and further predicted it at the global scale. In our

81 predicted map, we did not remove cropland or other heavily influenced areas (e.g., cities and roads), so the predicted map

82 represents a potential natural background without direct anthropogenic influence. With our enlarged dataset and our map of

83 global soil P distribution, we addressed the following research questions: (1) Which factors are the most important for

84 predicting the spatial variation of soil total P concentration in the top 1 m of soil? (2) How does soil total P concentration differ

85 among regions and soil layers? and (3) How large is the global total P stock in the top 1 m of soil?

86 **2 Material and Methods**

87 **2.1 Data source and processing**

88   Given massive measurements of soil total P concentration in literature, it is practically infeasible to collect all the

89 measurements in literature. Therefore, we collected soil total P concentration measurements in (semi-)natural terrestrial

90 ecosystems mainly from existing global or regional databases, and additionally from literature with focus on the

91 underrepresented regions identified in global databases, to ensure a good coverage of global terrestrial ecosystems. We defined

92 (semi-)natural ecosystems as ecosystems without any documented significant anthropogenic activities such as tillage,

93 fertilization, and heavy grazing. Forests with a stand age greater than 10 years were considered as (semi-)natural ecosystems.

94   We carefully checked the description of soil sampling in every cited paper for any anthropogenic activities such as tillage,

95   fertilization, and heavy grazing, and excluded such samples. Despite our efforts to exclude soils affected by anthropogenic

96   activities, some soils in our database might be influenced by undocumented anthropogenic activities (e.g., P fertilization in

97   reforested lands), particularly in Western Europe and Eastern USA (e.g., De Schrijver et al., 2012). We compiled the database

98   in four steps, which are described as follows.

99   First, we searched existing global or regional databases that may include soil total P concentration measurements in

100   (semi-)natural ecosystems in the Web of Science using key words "global OR terrestrial OR meta-analysis" AND "soil

101   phosphorus" NOT "crop OR agriculture" in topic. This search returned 714 papers by 15th September, 2020. After excluding

102   site-level studies and studies with artificial treatments (e.g., treatment with fertilizer, elevated temperature, or elevated

103   CO_2), 163 papers were retained. We then checked the main text, and the supplementary files, if available, of the 163 papers

104   to identify databases with soil total P concentration measurements. Seven databases with soil total P measures from seven

105   studies were selected. As observations in two databases (i.e., Li et al., 2014; Xu et al., 2013) were included in another database

106   (i.e., Wang et al., 2021), we finally used five databases (i.e., Wang et al., 2021; Hou et al., 2020; Hou et al., 2018b; Deng et al.,

107   2017; Augusto et al., 2017) and found 2591 observations in this step, as described in detail in Table S1.

108   Second, we used "soil phosphorus" as keywords to search global or regional databases stored in public data repositories

109   on 10th October, 2020, including Figshare (https://figshare.com/categories/Earth and Environmental Sciences/33), Earthdata

110   (https://earthdata.nasa.gov/), PANGAEA (https://www.pangaea.de/), Data.world (https://data.world/), Dryad

111   (https://datadryad.org/stash/), and Zenodo (https://zenodo.org/). We firstly screened the databases by titles, and then picked

112   out 80 potentially useful databases which were checked further by looking into the databases. There were nine databases with

113   soil total P concentration in (semi-)natural terrestrial ecosystems. Among the nine databases, five (Ji et al., 2018; Tipping et

114   al., 2016; McGroddy, 2012; Baribault et al., 2012; Cross, 1989) were excluded, due to a lack of specific site coordinates (i.e.,

115   longitude and latitude), which are needed to fill missing values of predictors from their global maps. In this step, 210

116   observations from four databases (i.e., Adams et al., 2020; Deiss et al., 2018; Yan et al., 2018; Gama-Rodrigues et al., 2014)

117   were collected.

118   Third, we included 1693 measurements of soil total P concentration in a global database of soil extractable P concentration

119   (Hou et al., unpublished), and 262 measurements of soil total P concentration in a global database of soil P fractions (He et al.,

120   unpublished). Original data sources of the two databases are given in Supplementary Text 1. After step 3, we combined

121   measurements collected in steps 1-3 and deleted 22 duplicated ones (i.e., measurements with the same site coordinates and soil

122   total P concentration), resulting in a total of 4734 site-level measurements of soil total P concentration from 11 databases listed

123   in Table S1.

124   Fourth, we searched additional soil total P concentration measurements from underrepresented regions identified in steps

125 1-3, from Web of Science using keywords of "soil phosphorus" along with the keywords of the underrepresented regions (listed

126 in detail in Table S2). According to criteria above, we only collected soil total P concentration measurements in (semi-)natural

127 terrestrial ecosystems. In this step, we collected 541 additional site-level measurements of soil total P concentrations from 60

128 additional papers (Table S2; Supplementary Text 1).

129 Following these steps, our database included 5,275 measurements of soil total P concentration at 1,894 sites from 761

130 studies (Supplementary Text 1 and Fig. S1), with 4,536 measurements in top 30 cm and 739 measurements in deeper soil

131 (depth > 30 cm). Besides soil total P concentration and site coordinates, we also included climate variables (i.e., MAT and

132 MAP), vegetation type, soil physiochemical properties (e.g., SOC, soil clay and sand contents, soil pH) in our database,

133 whenever available.

134
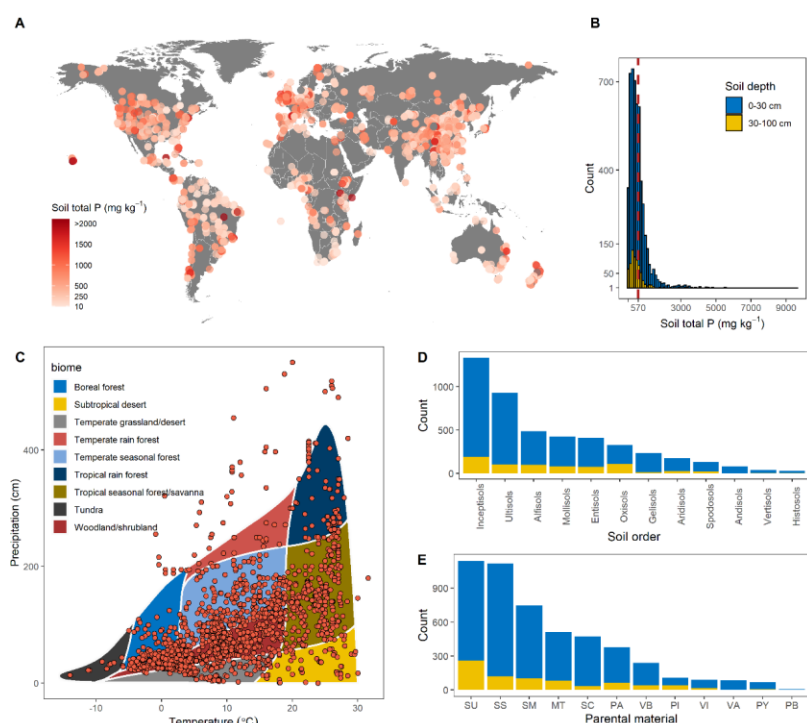
135 **Fig. 1 The distribution of our site-level training data.** The database contains 5,275 observations (A & B) covering all major terrestrial

136 biomes (C), 12 soil orders (D), and 12 parent materials (E). Red dashed line in figure (B) indicates the arithmetic mean of the soil total P

137 concentration (570 mg kg^{-1}). The abbreviations in figure (E) represent the following: SS: Siliciclastic sedimentary; SU: Unconsolidated

138 sediments; SM: Mixed sedimentary; MT: Metamorphics; SC: Carbonate sedimentary; PA: Acid plutonic; VB: Basic volcanic; VI:

139 Intermediate volcanic; PI: Intermediate plutonic; VA: Acid volcanic; PY: Pyroclastics; PB: Basic plutonic.

140 Soil total P concentration is thought to be influenced by five soil-forming factors, which are parent material, climate,

141 vegetation productivity, topography, and soil age (Delgado-Baquerizo et al., 2020; Jenny, 1941; Dokuchaev, 1883). Four of

142 the five factors were directly considered here (Table 1): parent material, climate (i.e. mean annual temperature (MAT), mean

143 annual precipitation (MAP), and biome), vegetation (i.e. net primary production (NPP)), and topography (e.g. slope and

144 elevation). As soil age was rarely reported, we used USDA soil orders as a proxy for age with 3 classes: slightly, intermediately,

145 and strongly weathered (Yang et al., 2013; Smeck, 1985). Among the 12 USDA soil orders, Entisols, Inceptisols, Histosols,

146 Andisols, and Gelisols are classified as slightly weathered soils. Alfisols, Mollisols, Aridisols, and Vertisols are classified as

147 intermediately weathered soils. Oxisols, Ultisols, and Spodosols are classified as strongly weathered soils (Yang et al., 2013;

148 Smeck, 1985). Moreover, we have classified each soil in our database according to soil types of the World Reference Base for

149 Soil Resources (WRB) (Table S3). We extracted WRB soil type of each site from a global WRB soil type map (Hengl et al.,

150 2017b) based on the geographical coordinates.

151 **Table 1 Summary of training data used to predict soil total P concentration.** P10 and P 90 indicate the percentile rank of 10% and 90%.

Group	Variables	Unit	Min.	P10	Mean	P90	Max.	PFL[*]	PFGM[#]
Climate	MAT	°C	-14	0.7	11.9	25.1	31.6	91%	9%
	MAP	mm	10	356	1146	2337	6576	91%	9%
Soil property	SOC	g kg^{-1}	0.1	2.6	41.3	92.8	545	81%	19%
	Soil pH		2.5	4.2	5.9	8.1	10.5	77%	23%
	Soil clay	g kg^{-1}	0.3	50	222	435	954	48%	52%
	Soil sand	g kg^{-1}	10	135	497	862	997	29%	71%
	Depth	cm	0.5	5	19.4	50	100	100%	0%
	Soil order		12 USDA soil orders					64%	36%
Parent material			13 parent materials					0%	100%
Vegetation	Biomes		6 major biomes					91%	9%
	NPP	kg C m^{-2}	<0.1	0.2	0.6	1.0	2.2	0%	100%
Topography	Slope	°	0	0	8.28	22	72	0%	100%
	Elevation	m	-41	34	861	2141	5175	67%	33%

152 MAT: Mean annual temperature; MAP: Mean annual precipitation; SOC: Soil organic carbon; NPP: Net primary production. * PFL:

153 Proportion from literature; # PFGM: Proportion from gridded map. PFL and PFGM indicate proportions of measurements from literature

154 and extracted from global gridded maps, respectively.

155 In addition to predictors of soil total P concentration related to soil-forming factors, we collected information about the

156 properties of the soils (e.g. soil organic carbon (SOC), soil pH, soil clay content (Clay) and soil sand content (Sand), and soil

157 depth (Depth); Table 1). These soil properties were used as additional predictors. We extracted predictors from each original

158 publication when available. In cases where information on predictors were not reported, we extracted the missing data from

159 gridded datasets (Table S3) based on the geographical coordinates of the measurement sites.

160 In the random forest model, correlated predictors can be substituted for each other, so that the importance of correlated

161 predictors will be shared, making the estimated importance smaller than the true value (Strobl et al., 2008). Thus, we did not

162 include soil total nitrogen content as it is correlated with SOC (r = +0.84), nor did we include aridity index as it is strongly

163 correlated with MAP (r = +0.82). We also did not include variables that were rarely reported in the referenced studies (e.g. soil

164 extractable aluminum and iron concentrations).

2.2 Statistical modelling

166 Among the 5,275 soil total P measurements, there were 15 extremely high values (> 4000 mg kg^{-1}) (Fig. 1B). These high
167 values were likely derived in exceptional geological contexts (Porder and Ramachandran, 2013), or special soils (e.g. very
168 young volcanic soils). We reported these extremely high values while summarizing the database, for example, in Table 2 and
169 Table 3. However, we excluded these 15 measurements from model training and correlation analyses to avoid their possible
170 large influences on the overall relationships between soil total P concentration and other variables.

171 We compared a suite of algorithms against the aforementioned 13 predictors which included three generalized linear
172 models, Cubist model, Boosted tree model, and random forest model (Table S4). Model performance was compared in terms
173 of R^2 and Root Mean Square Error (RMSE) (Minasny et al., 2017). A five-fold cross-validation method was used to evaluate
174 the performance of the models. In this method, the whole dataset was randomly split into five folds, each of which contained
175 20% of the data. One fold of data was used as test data, while the other four folds were used as training data. Then another fold
176 of data was used as test data, and the remaining ones as training data, and so on and so forth for a total of five times. Averages
177 of five sets of R^2 and RMSE were used as the model R^2 and RMSE, respectively. Based on the five-fold cross-validation
178 method, the random forest algorithm performed the best (R^2 = 0.65) among all five algorithms (Table S4) and was therefore
179 selected for follow-up analyses. Five-fold cross-validation was performed using the R package *caret* (v. 6.0-86) (Kuhn, 2020).
180 Random forest analysis was performed with the R package *caret* by applying the embedded R package *randomForest* version
181 3.1 (Liaw and Wiener, 2002) with an automated *mtry* parameter. The mean decrease in accuracy (%IncMSE) was used to
182 indicate the relative importance of each variable for predicting soil total P concentration. Partial dependence plots showed the
183 marginal effect of each continuous predictor on soil total P concentration.

184 Finally, we applied the above trained model to global databases of the 13 predictors to generate a global map of soil total
185 P concentration. The gridded driver variables used for the global prediction were all re-gridded to a spatial resolution of 0.05°
186 × 0.05° (the original resolution can be found in the Table S3). We did not remove cropland or other heavy influenced areas
187 (e.g. cities, roads, etc.), so the predicted map can be used to represent an initial state without direct anthropogenic influence.
188 Here we assume that cropland and other heavily influenced areas in their native states had the same set of relationships as for
189 (semi-)natural lands.

190 Soil depth was used as a covariate, so that the models could predict soil total P concentration for any given depth (Hengl
191 et al., 2017b). The partial dependence plot indicated that soil total P concentration approximately linearly decreased with soil
192 depth in the top 30 cm and there was no apparent trend with depth in the subsoil (~30-100 cm). Given this, we predicted global
193 soil total P concentration at 5 cm, 15 cm, 25 cm, and 65 cm to represent the soil total P concentration in the 0-10 cm, 10-20

194 cm, 20-30 cm, and 30-100 cm layers, respectively. Averages in other depth intervals (e.g. 0-30 cm or 0-100 cm), can be derived

195 by taking a weighted average of the predictions within the depth interval (Hengl et al., 2017b). We used global gridded soil

196 depth data (Shangguan et al., 2017) to correct the soil depth when it was less than 100 cm in any cell. The global soil P stock

197 maps for 0-10 cm, 10-20 cm, 20-30 cm, and 30-100 cm layers were calculated from the soil total P concentrations predicted

198 here and the soil bulk density in corresponding layers predicted by Hengl et al. (2017b).

199   Prediction uncertainty of each cell in the global gridded map was assessed using bootstrap samples with the quantile

200 regression forest technique (Meinshausen, 2006). Standard deviation was calculated to represent the uncertainty using

201 *quantregForest* function in the *quantregForest* R package (Meinshausen, 2017). Individual predictions of each tree in the

202 random forest model (n=500) were returned to assess the variation of predicted global mean soil total P concentration and

203 these results were used to assess the standard deviation of the estimated global soil P stock.

204   All statistical analyses and plotting were performed in the R environment (v. 4.0.2) (R Core Team, 2018).

3 Results

3.1 Characteristics of soil total P concentration across the world

207   Our soil total P concentration database included 5,275 measurements from 1,894 geographically distinct sites and covered

208 6 continents, all major biomes, and all 12 USDA soil orders in terrestrial ecosystems (Fig. 1A-D & Table S5). The database

209 was highly right-skewed (Fig.1B) and revealed that the soil total P concentration in natural soils of terrestrial ecosystems varied

210 from 1.4 to 9,636.0 mg kg^{-1}, with a mean, median and standard deviation of 570.0, 430.0, and 646.5 mg kg^{-1}, respectively

211 (Table 2). The database included soil total P concentration measurements from topsoil to 100 cm depth, with 84.4 % of the

212 measurements from the topsoil (e.g. 0-30 cm). The average soil total P concentration in our database was 583.7 and 495.2 mg

213 kg^{-1} in the topsoil (0-30cm) and subsoil (30-100 cm), respectively.

214 **Table 2 Soil total P concentration (mg kg^{-1}) in natural ecosystems for major biomes at 0-30 cm and 0-100 cm depth, respectively.**
215 Results based on our site-level database. P10, P25, P75, and P 90 indicate the percentile rank of 10%, 25%, 75%, and 90%.

	Min	P10	P25	Median	Mean	P75	P90	Max
0-30 cm								
Tundra	35.0	100.0	228.5	517.7	946.2	891.5	2016.4	9630.0
Boreal	3.0	99.9	317.2	571.0	705.2	879.5	1429.0	5520.0
Mediterranean	4.8	93.8	247.5	449.2	563.0	626.0	899.4	4433.0
Temperate	3.0	130.2	260.0	484.0	559.0	704.0	1037.4	4086.6
Tropics	3.4	73.0	146.6	293.0	439.0	531.5	968.7	3898.0
Desert	5.0	33.0	63.0	330.0	383.6	566.2	727.9	4800.0
Global	3.0	103.0	240.0	462.0	597.0	721.0	1100.0	9630.0
0-100 cm								
Tundra	35.0	104.7	253.8	550.1	984.8	1000.0	2222.0	9630.0

	Min	P10	P25	Median	Mean	P75	P90	Max
Boreal	3.0	116.3	327.5	560.0	723.3	864.8	1424.1	5520.0
Mediterranean	4.8	96.0	252.3	443.3	554.4	621.5	873.0	4433.0
Temperate	3.0	128.9	250.0	460.0	539.7	679.6	1008.6	4086.6
Tropics	1.4	63.0	140.0	284.0	421.2	529.0	922.0	3898.0
Desert	5.0	33.7	62.1	337.5	381.0	566.9	710.0	4800.0
Global	1.4	90.4	217.0	437.0	569.0	690.0	1070.0	9630.0

设置了格式: 字体颜色: 蓝色

Table 3 Soil total P concentration (mg kg⁻¹) in 12 USDA soil orders and three weathering stages at 0-30 cm and 0-100 cm depth, respectively. Results based on our database. P10, P25, P75, and P 90 indicate the percentile rank of 10%, 25%, 75%, and 90%.

	Min	P10	P25	Median	Mean	P75	P90	Max
0-30 cm								
Slightly weathered	11.0	145.4	295.3	552.0	721.0	850.0	1368.4	9630.0
Andisols	175.0	321.9	534.4	883.2	1042.4	1459.8	2040.9	3548.0
Geilsols	35.0	169.2	307.7	552.0	1116.5	990.0	2950.0	9630.0
Entisols	24.3	100.0	263.9	540.3	583.0	834.1	1090.0	2321.3
Inceptisols	11.0	143.1	285.4	536.3	654.8	812.2	1200.0	5520.0
Histosols	66.0	336.9	550.0	753.5	837.0	1029.7	1484.0	1711.0
Intermediately weathered	3.0	38.4	169.2	390.0	492.7	630.0	1019.8	4800.0
Aridisols	5.0	34.1	180.0	396.7	450.7	600.0	805.8	4800.0
Alfisols	3.0	29.8	133.6	352.5	495.5	639.4	1160.9	4243.0
Mollisols	9.8	53.3	213.9	420.5	462.0	627.6	848.6	3199.0
Vertisols	112.7	202.6	243.0	480.0	923.2	1087.0	2870.0	3680.0
Strongly weathered	3.4	104.7	220.0	390.0	483.6	613.8	912.0	4086.6
Oxisols	5.1	79.0	128.0	333.5	400.5	518.3	912.3	2000.0
Ultisols	3.4	129.8	246.6	406.0	491.2	607.8	870.0	4086.6
Spodosols	14.5	145.8	270.0	436.5	591.4	751.5	1124.2	3444.2
0-100 cm								
Slightly weathered	11.0	144.6	296.1	547.6	719.4	838.6	1362.4	9630.0
Andisols	175.0	321.9	534.4	883.2	1042.4	1459.8	2040.9	3548.0
Geilsols	35.0	175.1	321.8	584.1	1145.8	1047.7	3013.0	9630.0
Entisols	14.1	80.0	246.3	515.7	551.0	800.0	1030.0	2321.3
Inceptisols	11.0	150.4	292.0	530.8	667.7	805.8	1240.0	5520.0
Histosols	66.0	341.4	550.0	800.0	877.0	1061.4	1686.0	1996.0
Intermediately weathered	1.4	41.2	191.3	390.0	481.1	612.6	965.0	4800.0
Aridisols	5.0	35.9	175.0	395.7	446.8	590.5	806.6	4800.0
Alfisols	1.4	27.1	141.4	325.2	470.1	610.0	1072.5	4243.0
Mollisols	9.8	76.1	261.1	457.4	470.3	622.3	838.2	3199.0
Vertisols	112.7	199.6	242.0	421.8	871.5	1012.5	2825.0	3680.0
Strongly weathered	3.4	103.9	210.0	377.1	472.3	597.3	900.0	4086.6
Oxisols	5.1	89.1	141.0	360.5	435.9	625.0	950.8	2000.0
Ultisols	3.4	111.7	219.5	380.0	466.6	582.8	837.0	4086.6
Spodosols	14.5	149.1	262.4	424.0	597.9	731.0	1138.9	3444.2

设置了格式: 字体颜色: 蓝色

The database revealed that soil total P concentration varied within and among biomes. The soil from tundra and boreal biomes had the highest soil total P concentrations. Mediterranean and temperate soils had intermediate soil total P

222 concentrations. Soils in the desert and tropics had relatively lower soil total P concentrations (Table 2 & Fig. 2B). Soil total P

223 concentration also varied with different soil orders (Table 3). Soil total P concentration decreased from slightly weathered soil

224 (mean value 719.4 mg kg^{-1}) to intermediately and strongly weathered soils (mean values of 481.1 mg kg^{-1} and 472.3 mg kg^{-1},

225 respectively) (Fig. 2C). The declining trend of soil total P during soil development supports the Walker and Syers (1976)

226 conceptual model of phosphorus dynamics during long-term ecosystem development. And this pattern is consistent with

227 previous studies (i.e., Cross and Schlesinger, 1995; Yang et al., 2011; Yang et al., 2013). Relationship between soil total P

228 concentration and different World Reference Base for Soil Resources (WRB) soil types can be found in the supplementary file

229 (Table S6).

230

231
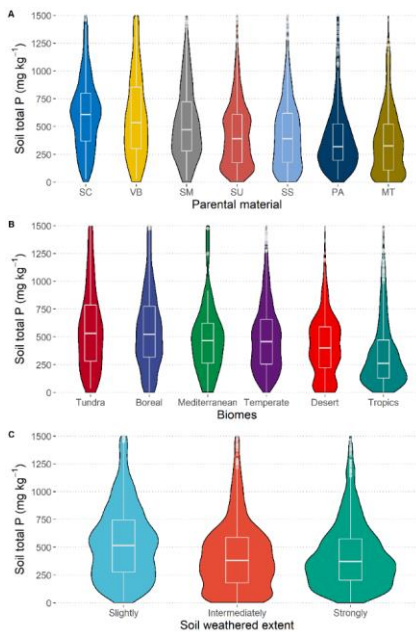
232 **Fig. 2 Soil total P concentration in relation to parent material, biome, and soil weathering extent.** For visualization, we chose to limit
233 the y-axis to 1500 mg kg^{-1}; and in panel A, only parent material types with more than 100 measurements in our database were shown; the
234 abbreviations in figure (A) represent the following: SC: Carbonate sedimentary; VB: Basic volcanic; SM: Mixed sedimentary; SU:
235 Unconsolidated sediments; SS: Siliciclastic sedimentary; PA: Acid plutonic; MT: Metamorphics.

236 **3.2 Model performance and drivers of soil total P concentration**

237 The random forest regression model explained 65% of soil total P concentration variability across all sites, with an RMSE

238 of 288.8 mg kg^{-1} (Fig. 3B & Table S4). The random forest model revealed that the two most important predictors of soil total

239 P concentration were SOC content and parent material. The remaining predictors showed a lower, but non-negligible influence,

240 with MAT and soil sand content having the most noticeable influence (Fig. 3A). Although soil order, biome, elevation, slope,

241 depth, NPP, and pH showed significant influences on soil total P concentration (Fig. 2 and Fig. S3), their relative importance

242 was lower than the above four predictors. Partial dependent plots (Fig. 4) revealed similar results to Pearson correlation analysis

243 (Fig. S3). The partial dependent plots indicated a significant and positive relationship between soil total P concentration and

244 SOC at a global scale; soil total P concentration was significantly and negatively correlated with MAT and soil sand content

245 (Fig. S4). The Pearson correlation indicated the correlation coefficients between soil total P concentration and the top three

246 continuous predictors MAT, SOC, and soil sand content were -0.23, 0.19, and -0.18, respectively (Fig. S3).

247
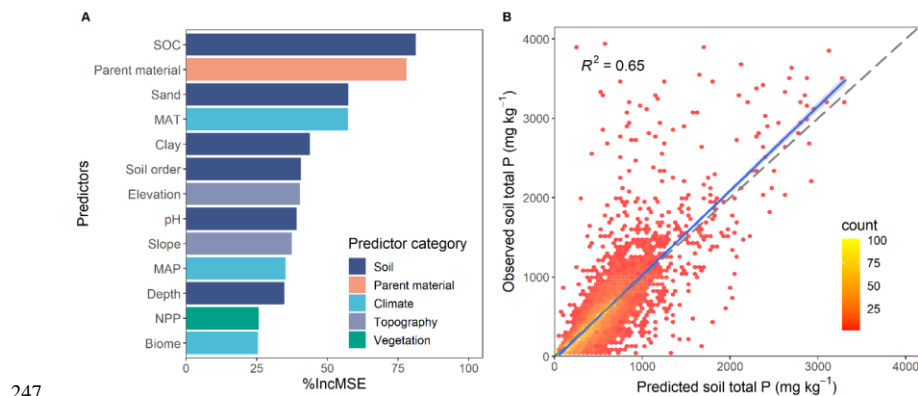
248 **Fig. 3 Results of the random forest model predicting soil total P concentration.** (A) The relative importance of predictors in the model.

249 (B) Predicted vs. observed soil total P concentration; the dashed line indicates the 1:1 line; the blue line indicates the regression line between

250 predicted and observed values.
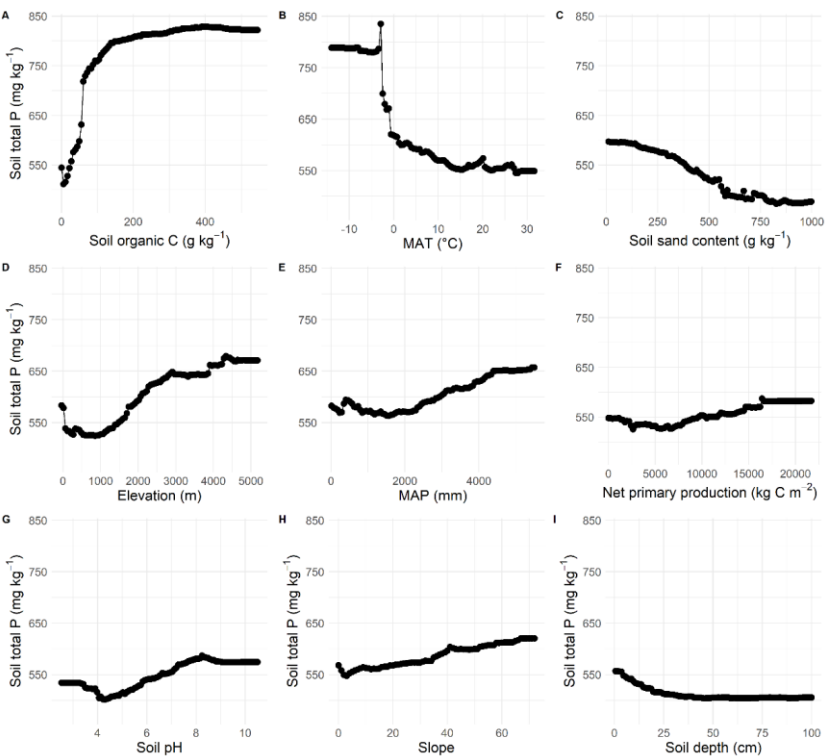
251
252 **Fig. 4 Partial dependence plots showing the dependence of soil total P concentration on predictors.** Soil total P concentration in relation
253 to SOC concentration, MAT, soil sand content, elevation, MAP, net primary production, soil pH, slope, and soil depth (A, B, C, D, E, F, G,
254 H, I, respectively).

255 **3.3 Global patterns of soil total P**

256   In our predicted global map (Fig. 5), we did not remove cropland or other heavily influenced areas (e.g., cities and roads),
257 so the predicted map can be used to represent a natural background without direct anthropogenic influence. The predicted soil
258 total P indicated that the total global P stocks in the topsoil (0-30 cm) and subsoil (30-100 cm) were 26.8 (standard deviation
259 = 3.1) Pg and 62.2 (standard deviation = 8.9) Pg, respectively (excluding Antarctica; Table 4). Estimated area-weighted average
260 soil total P concentrations in the topsoil and subsoil were 529.0 and 502.3 mg kg^{-1}, respectively. Estimated area-weighted
261 average soil total P content in the topsoil and subsoil were 209.7 and 487.0 g cm^{-2}, respectively.

262 **Table 4 Analysis of the predicted global map of soil total P.** Area weighted average soil total P concentration was calculated based on our
263 predicted map. Converting soil total P concentration to soil total P content and stock used the soil bulk density (Hengl et al., 2017b) and land
264 area.

0-30 cm	30-100 cm

Continent	Soil total P concentration (mg kg⁻¹)	Soil total P content (g m⁻²)	Soil P stock (Pg)	Soil total P concentration (mg kg⁻¹)	Soil total P content (g m⁻²)	Soil P stock (Pg)
Africa	390.2	164.1	4.5	360.7	362.8	10.1
Asia	603.0	238.7	10.3	576.3	565.2	24.3
Europe	632.4	240.9	2.4	601.1	581.7	5.7
Oceania	401.5	177.1	1.4	373.4	397.6	3.4
South America	411.5	158.1	2.8	392.0	358.6	6.3
North America	657.3	251.2	5.3	631.5	587.4	12.3
Global	529.0	209.7	26.8	502.3	487.0	62.2

The estimated global map of soil total P concentration revealed latitudinal patterns (Fig. 5), which were also found from analysis of the site-level data (Fig. S4K). Soil total P concentration significantly increased from the equator to the poles in both hemispheres (P<0.001). The latitudinal pattern of soil total P concentration was not found in earlier work aiming at extrapolating global soil P measurements to global scale (Yang et al., 2013; Shangguan et al., 2014). Our predicted soil total P concentrations were weakly correlated, though significantly, with earlier predicted maps, i.e., Yang et al. (2013) and Shangguan et al. (2014) (Fig. S6).

Highlands and mountains at low latitudes (e.g., the Tibetan plateaus, Andes, Africa highlands, west India etc.) had high soil total P concentrations. Our map also indicated some regional difference in soil total P, for example, central Australia was low in soil total P compared with east and west Australia. On a larger scale, South America, Oceania, and Africa had the lowest soil total P concentration, while soil total P concentration was highest in Europe, North America, and Asia (Table 4). The estimated soil total P concentrations in the subsoil showed similar patterns to those found in the topsoil (Fig. 5A&C).
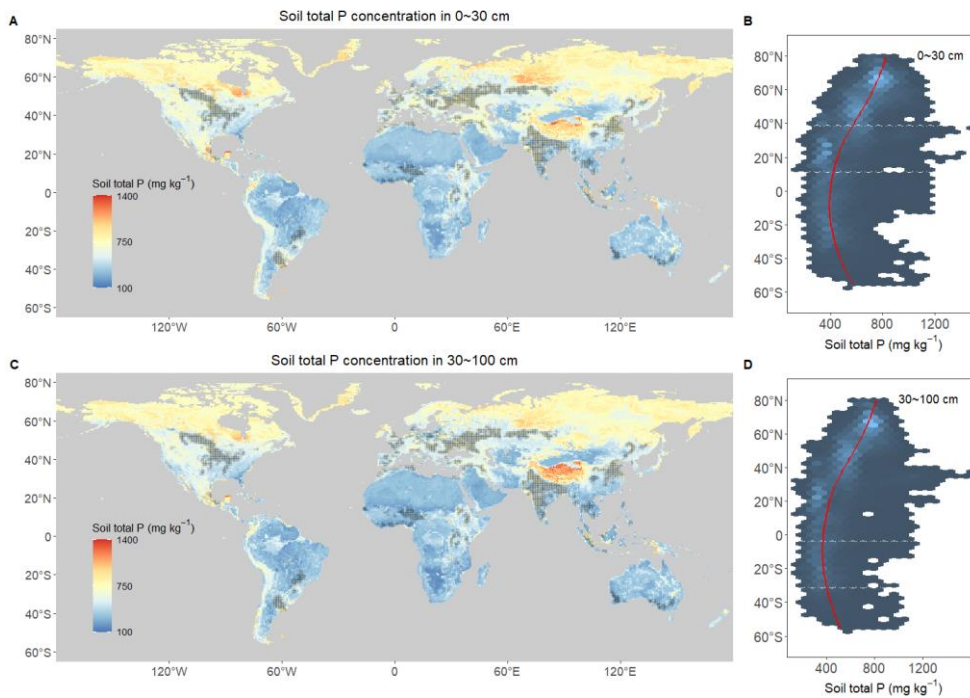
278 **Fig. 5 Global maps of total P concentration in the 0-30 cm and 30-100 cm of soils.** A and B are maps of topsoil (0-30 cm) total P
279 concentration and the latitudinal patterns, respectively. C and D are maps of subsoil (30-100 cm) total P concentration and the latitudinal
280 patterns, respectively. Red lines in B and D indicate the locally weighted regressions between latitude and soil total P concentration in the
281 precited global map. Note that we did not remove cropland or any other heavy influenced areas from the predicted maps, so they can be used
282 to represent soils without essential anthropogenic activities. In this figure, we used "x" to indicate grid-cells with more than 50% of areas
283 comprised by cropland. A map without the cropland symbols is visible in the Fig. S7.

284 **4 Discussion**

285   With our soil total P concentration dataset, we quantified soil total P concentration in natural ecosystems, identified its key

286 drivers, and predicted it for terrestrial ecosystems globally. Our work goes beyond previous studies (Delmas et al., 2015; Hengl

287 et al., 2017a; Shangguan et al., 2014; Viscarra Rossel and Bui, 2016; Yang et al., 2013; Cheng et al., 2016) which used limited

288 data that did not represent the heterogeneous conditions found on Earth well, and did not separate natural soils from human-

289 managed soils and therefore may not be able to distinguish natural drivers from anthropogenic factors (e.g. land use type,

290 mineral fertilizer). In addition, we mapped soil total P concentration by considering more predictors, at multiple soil depths,

291 and at a higher resolution than previous studies.

292 **4.1 Characteristics of soil total P concentration**

293   Given the larger number of measurements that we considered, the range of total P concentration in our study (1.4–9630.0

294 mg kg^{-1}) is wider than that reported in Cleveland and Liptzin (2007) (83.7–2746.6 mg kg^{-1}; n=186), Xu et al. (2013) (12.7–

295 8400.1 mg kg^{-1}; n=536), Li et al. (2014) (30– 2744 mg kg^{-1}; n=178), and Hou et al. (2018b) (4.8–2157.0 mg kg^{-1}; n=254). The

296 average soil total P concentration in our site-level database (570.0 mg kg^{-1}) was within the range of previous estimates by

297 Cleveland and Liptzin (2007) (721.1 mg kg^{-1}), Xu et al. (2013) (756.4 mg kg^{-1}), Li et al. (2014) (463.6 mg kg^{-1}), and Hou et

298 al. (2018b) (471.9 mg kg^{-1}).

299 **4.2 Soil total P concentration in relation to its predictors**

300 In agreement with previous studies, soil total P concentration was largely predicted by parent material type (Deiss et al.,

301 2018; Augusto et al., 2017; Porder and Ramachandran, 2013). This result supports the use of parent material to map soil total

302 P concentration at the global scale (Yang et al., 2013). Parent material can affect soil total P concentration both directly and

303 indirectly. Some parent materials tend to have higher P concentrations, which then translates into higher total soil P (Mage and

304 Porder, 2013; Dieter et al., 2010; Kitayama et al., 2000). Additionally, parent material also affects soil total P indirectly via the

305 influence of soil physiochemical properties such as soil texture, pH, and Al and Fe oxides (Siqueira et al., 2021; Mehmood et

306 al., 2018). For example, the retention of P in soil can be influenced by the soil content of clay, soluble calcium, and Fe

307 oxyhydroxides (Delgado-Baquerizo et al., 2020; Mehmood et al., 2018; Achat et al., 2016b). As such, parent material type is

308 a critical predictor of soil total P from local to global scales.

309 Interestingly, we found that SOC was one of the two most important predictors of soil total P concentration. The positive

310 relationship between soil total P and SOC has two possible explanations. First, this relationship may reflect the coupling

311 between P and C in soils (Hou et al., 2018a) given that soil organic matter is characterized by a rather narrow range of C:P

312 ratio (Cleveland and Liptzin, 2007; Spohn, 2020; Tipping et al., 2016). Second, P and organic C are stabilized and retained

313 through similar processes in soil (Doetterl et al., 2015). For example, reactive minerals can simultaneously stabilize both P and

314 organic C in soil (Helfenstein et al., 2018). As such, the strong relationship between SOC and total P at the global scale confirms

315 that SOC is an integrated measure of biotic (e.g. soil microbial activity) and abiotic (e.g. cation exchangeable capacity) factors

316 that regulate soil total P (Spohn, 2020; Wang et al., 2020).

317 Consistent with a recent global synthesis that focused on soil P fractions (Hou et al., 2018a), our result indicated that MAT

318 was a more important predictor of soil total P concentration than MAP. The negative relationship could be because soils under

319 low MAT are often found at high latitudes where soils were eroded during the last glaciation. These soils tend to be much

320 younger compared to soils at low latitudes with high MAT and thus have experienced less losses of P (Vitousek et al., 2010).

321 In addition, high MAT and MAP generally promote soil weathering as well as plant growth and P uptake, resulting in the

322 depletion of soil P (Huston and Wolverton, 2009; Arenberg and Arai, 2019; Huston, 2012).

323 Further, we provide two explanations for the negative relationship between soil total P concentration and sand content.

324 First, soil sand content is a surrogate for quartz content (Bui & Henderson, 2013), and the rock content in quartz is usually

325 negatively correlated with the total P content of siliceous rocks (Hahm et al., 2014; Vitousek et al., 2010). Second, soil sand is

326 worse at retaining nutrients including P than other soil fractions (Augusto et al., 2017). For example, loamy soils regularly lose

327 0.3–0.5 kg P ha^{-1} yr^{-1} by leaching, while coarse sandy soils lose up to 2.0 kg P ha^{-1} yr^{-1} (Amberger, 1996).

4.3 Global patterns of soil total P

329 Based on our predicted global map, we estimated that the area-weighted global average of soil total P concentration was

330 529.0 and 502.3 mg kg^{-1} in the topsoil (0-30 cm) and subsoil (30-100 cm), respectively. Our estimated of the area-weighted

331 average soil total P in the topsoil was higher than previous estimates by Yang et al. (2013) (374.7 mg kg^{-1}) and Shangguan et

332 al. (2014) (484.7 mg kg^{-1}), but was very close to the estimate by Xu et al. (2013) (514.6 mg kg^{-1}). Our estimate of the global

333 soil P stock in the top 30 cm of soil (26.8 Pg; excluding Antarctica) was in line with the estimate of Shuanguan et al. (2013)

334 (26.7 Pg in the top 30 cm), but was higher than the estimates of Yang et al. (2013) (24.4 Pg in the top 30 cm), Wang et al.

335 (2010) (18.2 Pg in the top 30 cm), and Smil (2000) (24 Pg). Additionally, our estimate was much lower than a much earlier

336 estimate by Butcher et al. (1992) (about 120 Pg in the top 30 cm).

337 Our predicted soil total P concentrations decreased significantly with decreasing latitude in both hemispheres. This result

338 is consistent with our theoretical understanding of the evolution of soils in soil chronosequences (Walker and Syres 1976) and

339 the stark differences in soil age and weathering intensity between low and high latitude regions. And this result is agreement

340 with a recent meta-analysis that revealed P-limitation to plant growth decreased significantly with latitude (Hou et al., 2021).

341 Lowland tropical soils tend to be more weathered compared to soils at high latitudes due to warmer and more humid

342 climate which promotes weathering (Hou et al., 2018a). Moreover, the last glaciation could have eroded soils at norther

343 higher latitude and have caused relatively young and P-enriched soils (Vitousek et al., 2010; Reich and Oleksyn, 2004).

344 Our result is consistent with Xu et al. (2013); by comparing soil total P concentration across the major biomes, the authors

345 found the highest soil total P concentration in the tundra and the lowest in the tropical/subtropical forest. Previous global maps

346 of soil total P concentration were not able to capture the latitudinal trend of soil total P concentrations (Yang et al., 2013;

347 Shangguan et al., 2014), likely due to poorer spatial coverage of their measurements. For example, their measurements were

348 mostly from the US and China, with a very small proportion of measurements from high latitudes.

349 While we found a latitudinal gradient in soil total P concentration, heterogeneity in soil total P concentration at the regional

350 and local scales was large. For example, consistent with Brédoire et al. (2016), we found that the soil total P concentration was

351 higher in Siberia than in northern Europe, both of which have similar latitudes. First, this difference may be due to the fact that

352 glaciation was more regular and intense in Siberia than in northern Europe (Wassen et al., 2021), leading to a more intensive

353 rejuvenation of soils. Second, the warmer and wetter climate in northern Europe may promote weathering which releases P

354 from parent material (Goll et al., 2014) and makes it subject to loss (Fig. S8). Regional variation in soil total P concentration

355 may also be attributable to regional variation in parent material. For example, higher soil total P concentration in eastern

356 Australia than in central Australia was probably due to P-enriched basaltic lithologies in eastern Australia (6500–8700 mg kg^{-1})

357 (Viscarra Rossel and Bui, 2016). Moreover, regional differences in soil total P concentration may be related to topography

358 conditions. For example, higher soil total P concentration in the Tibetan plateau than in eastern China may be the result of

359 higher elevation and lower MAT in the Tibetan plateau (Zhang et al., 2005).

360 **4.4 Limitation and prediction uncertainty**

361   Despite our unprecedented effort to construct a database and perform global predictions, our study has some limitations.

362 First, some regions were still underrepresented, e.g., northern Canada, Russia, middle Asia, and inner Australia, which may

363 result in a low accuracy of predicted values in these regions (Ploton et al., 2020). Further, our assumption that soils which are

364 or have been in agricultural use can be characterized in their native state by the same relationships as semi(natural) soils might

365 not hold true. For example, as fertile soils are preferred in agriculture and forestry. Second, subsoils (> 30 cm depth) were not

366 well represented in our dataset (14%) and therefore predicted P concentrations of subsoils may suffer from larger uncertainties

367 than those of topsoils (< 30 cm depth). Third, some predictors were largely missing. Map-filled values suffer from large

368 uncertainties, especially for the soil variables. This may cause some uncertainties in the predicted soil total P concentration.

369 Finally, 36% of the variation in soil total P concentration was not explained, despite inclusion of 13 predictors using an

370 advanced machine learning approach. This result may be because of measurement errors and/or methodological constraints.

371 These limitations highlight the need for more measurements of subsoil total P concentration and closely associated variables,

372 especially from the underrepresented regions, as well as more advanced statistical methods for spatial predictions.

373 **5 Conclusion**

374   By constructing a database of total P concentration globally, we quantified the relative importance of multiple soil-forming

375 variables for predicting soil total P concentration and further estimated it at the global scale. Our results indicated that no single

376 variable can be used to predict soil total P concentration. Instead, it is a combination of variables that are needed to reliably

377 predict soil total P concentration, among which SOC, parent material, MAT, and soil sand content are the most important

378 predictors. Soil total P concentration was positively correlated with SOC and negatively correlated with both MAT and soil

379 sand content. Our predicted map captures the latitudinal gradient in potential soil total P concentration expected from our

380 theoretical understanding. We estimated that P stocks in the topsoil (0-30 cm) and subsoil (30-100 cm) of soil of natural

381 ecosystems (excluding Antarctica) were 26.8 and 62.2 Pg, respectively. Our improved global map of soil total P will be an

382 important resource for future work which aims to tackle issues related to P cycling, including predicting future land carbon

383 sink potential and P losses to aquatic and marine ecosystems as well as modeling the P needs of crops to increase food security.

384

385 **Data availability**

386 Raw datasets, R code, and global maps generated in this study are available at https://doi.org/10.6084/m9.figshare.14583375

387 (He et al., 2021).

388 **Author contributions**

389 X.H. and E.H designed this study. X.H., E.H, L.A., and Z.W. collected the data. X.H., E.H., L.A., D.S.G., B.R., Y.W., J.H.,

390 Y.H., and K.Y. discussed analyzing methods. X.H. conducted the analysis and drafted the manuscript. All authors discussed

391 the results and contributed to the manuscript.

392 **Acknowledgements**

393 This research was funded by the National Natural Science Foundation of China (32071652, 31870464), the China Postdoctoral

394 Science Foundation (2020M673123), Chongqing Technology Innovation and Application Demonstration Major Theme

395 Special Project (cstc2018jszx-zdyfxmX0007), and the ANR CLAND Convergence Institute. We would like to thank Dr.

396 Morgan Furze at Yale University for his assistance with English language and grammatical editing.

397 **Competing interests**

398 The authors declare that they have no conflict of interest.

399

400

401

References

403 Achat, D.L., Augusto, L., Gallet-Budynek, A. and Loustau, D.: Future challenges in coupled C-N-P cycle models for terrestrial
404   ecosystems under global change: a review. Biogeochemistry, 131, 173-202, doi: 10.1007/s10533-016-0274-9, 2016a.

405 Achat, D.L., Pousse, N., Nicolas, M., Brédoire, F. and Augusto, L.: Soil properties controlling inorganic phosphorus
406   availability: general results from a national forest network and a global compilation of the literature. Biogeochemistry, 127,
407   255-272, https://doi.or/10.1007/s10533-015-0178-0, 2016b.

408 Adams, J., Tipping, E., Thacker, S.A. and Quinton, J.N.: Phosphorus, carbon and nitrogen concentrations in UK soil mineral
409   fractions, 2013-2014. NERC Environmental Information Data Centre, doi: 10.5285/e6e9a85c-b537-4110-899f-
410   2c1498bc826c, 2020.

411 Alewell, C., Ringeval, B., Ballabio, C., Robinson, D.A., Panagos, P. and Borrelli, P.: Global phosphorus shortage will be
412   aggravated by soil erosion. Nat. Commun., 11, 4546, doi: 10.1038/s41467-020-18326-7, 2020.

413 Amberger, A., Pflanzenernährung. Ökologische und physiologische Grundlagen, Dynamik und Stoffwechsel der
414   Nährelemente, 4th ed.. Eugen Ulmer, Stuttgart, [in German], 1996.

415 Andersson, H., Bergström, L., Djodjic, F., Ulén, B. and Kirchmann, H.: Topsoil and Subsoil Properties Influence Phosphorus
416   Leaching from Four Agricultural Soils. J. Environ. Qual., 42, 455-463, doi: 10.2134/jeq2012.0224, 2013.

417 Arenberg, M.R. and Arai, Y.: Uncertainties in soil physicochemical factors controlling phosphorus mineralization and
418   immobilization processes. Adv. Agron., 154, 153-200, doi: 10.1016/bs.agron.2018.11.005, 2019.

419 Augusto, L., Achat, D.L., Jonard, M., Vidal, D. and Ringeval, B.: Soil parent material—A major driver of plant nutrient
420   limitations in terrestrial ecosystems. Global Change Biol., 23, 3808-3824, doi: 10.1111/gcb.13691, 2017.

421 Augusto, L., Bakker, M.R., Morel, C., Meredieu, C., Trichet, P., Badeau, V., Arrouays, D., Plassard, C., Achat, D.L., Gallet-
422   Budynek, A., Merzeau, D., Canteloup, D., Najar, M. and Ranger, J.: Is 'grey literature' a reliable source of data to
423   characterize soils at the scale of a region? A case study in a maritime pine forest in southwestern France. Eur. J. Soil Sci.,
424   61, 807-822, doi: 10.1111/j.1365-2389.2010.01286.x, 2010.
425 Ballabio, C., Lugato, E., Fernández-Ugalde, O., Orgiazzi, A., Jones, A., Borrelli, P., Montanarella, L. and Panagos, P.:
426   Mapping LUCAS topsoil chemical properties at European scale using Gaussian process regression. Geoderma, 355,
427   113912, doi: 10.1016/j.geoderma.2019.113912, 2019.
428 Baribault, T.W., Kobe, R.K. and Finley, A.O.: Data from: Tropical tree growth is correlated with soil phosphorus, potassium,
429   and calcium, though not for legumes, Dryad, Dataset, doi: 10.5061/dryad.r9p70, 2012.
430 Brédoire, F., Bakker, M.R., Augusto, L., Barsukov, P.A., Derrien, D., Nikitich, P., Rusalimova, O., Zeller, B. and Achat, D.L.:
431   What is the P value of Siberian soils? Soil phosphorus status in south-western Siberia and comparison with a global data
432   set. Biogeosciences, 13, 2493-2509, doi: 10.5194/bg-13-2493-2016, 2016.
433 Beusen, A.H.W., Van Beek, L.P.H., Bouwman, A.F., Mogollón, J.M. and Middelburg, J.J.: Coupling global models for
434   hydrology and nutrient loading to simulate nitrogen and phosphorus retention in surface water – description of
435   IMAGE – GNM and analysis of performance. Geosci. Model Dev., 8, 4045-4067, doi: 10.5194/gmd-8-4045-2015, 2015.
436 Buendía, C., Kleidon, A. and Porporato, A.: The role of tectonic uplift, climate, and vegetation in the long-term terrestrial
437   phosphorous cycle. Biogeosciences, 7, 2025-2038, doi: 10.5194/bg-7-2025-2010, 2010.
438 Bui, E.N. and Henderson, B.L.: C:N:P stoichiometry in Australian soils with respect to vegetation and environmental factors.
439   Plant Soil, 373, 553-568, doi: 10.1007/s11104-013-1823-9, 2013.
440 Butcher, S.S., Charlson, R.J., Orians, G.H. and Wolfe, G.V., Global Biogeochemical Cycles. Academic Press (Harcourt
441   Brace Jovanovich), London, 1992.
442 Cheng, Y., Li, P., Xu, G., Li, Z., Cheng, S. and Gao, H.: Spatial distribution of soil total phosphorus in Yingwugou watershed
443   of the Dan River, China. Catena, 136, 175-181, doi: 10.1016/j.catena.2015.02.015, 2016.
444 Cheng, Y., Li, P., Xu, G., Li, Z., Yu, K., Cheng, S., Zhao, B. and Wang, F.: Factors that influence soil total phosphorus sources
445   on dam fields that are part of ecological construction programs on the Loess Plateau, China. Catena, 171, 107-114, doi:
446   10.1016/j.catena.2018.07.006, 2018.
447 Cleveland, C.C. and Liptzin, D.: C:N:P stoichiometry in soil: is there a "Redfield Ratio" for the microbial biomass?
448   Biogeochemistry, 85, 235-252, doi: 10.1007/s10533-007-9132-0, 2007.
449 Cross, A.: Phosphorus fractions in grassland and shrubland soils at the Sevilleta NWR sev.149.2
450   (https://knb.ecoinformatics.org/knb/metacat/sev.149.2/default).,1989.
451 Cross, A.F. and Schlesinger, W.H.: A literature review and evaluation of the. Hedley fractionation: Applications to the
452   biogeochemical cycle of soil phosphorus in natural ecosystems. Geoderma, 64, 197-214, doi: 10.1016/0016-
453   7061(94)00023-4, 1995.
454 De Schrijver, A., Vesterdal, L., Hansen, K., De Frenne, P., Augusto, L., Achat, D.L., Staelens, J., Baeten, L., De Keersmaeker,
455   L., De Neve, S. and Verheyen, K.: Four decades of post-agricultural forest development have caused major redistributions
456   of soil phosphorus fractions. Oecologia, 169, 221-234, doi: 10.1007/s00442-011-2185-8, 2012.
457 Deiss, L., de Moraes, A. and Maire, V.: Environmental drivers of soil phosphorus composition in natural ecosystems.
458   Biogeosciences, 15, 4575-4592, doi: 10.5194/bg-15-4575-2018, 2018.
459 Delgado-Baquerizo, M., Reich, P.B., Bardgett, R.D., Eldridge, D.J., Lambers, H., Wardle, D.A., Reed, S.C., Plaza, C., Png,
460   G.K., Neuhauser, S., Berhe, A.A., Hart, S.C., Hu, H., He, J., Bastida, F., Abades, S., Alfaro, F.D., Cutler, N.A., Gallardo,
461   A., García-Velázquez, L., Hayes, P.E., Hseu, Z., Pérez, C.A., Santos, F., Siebe, C., Trivedi, P., Sullivan, B.W., Weber-
462   Grullon, L., Williams, M.A. and Fierer, N.: The influence of soil age on ecosystem structure and function across biomes.
463   Nat. Commun., 11, 4721-4721, doi: 10.1038/s41467-020-18451-3, 2020.
464 Delmas, M., Saby, N., Arrouays, D., Dupas, R., Lemercier, B., Pellerin, S. and Gascuel-Odoux, C.: Explaining and mapping
465   total phosphorus content in French topsoils. Soil Use Manage., 31, 259-269, doi: 10.1111/sum.12192, 2015.
466 Deng, Q., McMahon, D.E., Xiang, Y., Yu, C.L., Jackson, R.B. and Hui, D.: A global meta-analysis of soil phosphorus
467   dynamics after afforestation. New Phytol, 213, 181-192, doi: 10.1111/nph.14119, 2017.

468 Dieter, D., Elsenbeer, H. and Turner, B.L.: Phosphorus fractionation in lowland tropical rainforest soils in central Panama.
469   Catena, 82, 118-125, doi: 10.1016/j.catena.2010.05.010, 2010.

470 Doetterl, S., Stevens, A., Six, J., Merckx, R., Van Oost, K., Casanova Pinto, M., Casanova-Katny, A., Muñoz, C., Boudin, M.,
471   Zagal Venegas, E. and Boeckx, P.: Soil carbon storage controlled by interactions between geochemistry and climate. Nat.
472   Geosci., 8, 780-783, doi: 10.1038/ngeo2516, 2015.

473 Dokuchaev, V.V., The Russian chernozem. St. Petersburg, Russia: Imperial Univ. of St. Petersburg. Report to the Free
474   Economic Society. [in Russian], 1883.

475 Elser, J.J., Bracken, M.E.S., Cleland, E.E., Gruner, D.S., Harpole, W.S., Hillebrand, H., Ngai, J.T., Seabloom, E.W., Shurin,
476   J.B. and Smith, J.E.: Global analysis of nitrogen and phosphorus limitation of primary producers in freshwater, marine and
477   terrestrial ecosystems. Ecol. Lett., 10, 1135-1142, doi: 10.1111/j.1461-0248.2007.01113.x, 2007.

478 Fleischer, K., Rammig, A., Kauwe, D.M.G., Walker, A.P., Domingues, T.F., Fuchslueger, L., Garcia, S., Goll, D.S., Grandis,
479   A., Jiang, M., Haverd, V., Hofhansl, F., Holm, J.A., Kruijt, B., Leung, F., Medlyn, B.E., Mercado, L.M., Norby, R.J., Pak,
480   B., Randow, V.C., Quesada, C.A., Schaap, K.J., Valverde-Barrantes, O.J., Wang, Y.P., Yang, X., Zaehle, S., Zhu, Q.,
481   Lapola, D.M. and Oak Ridge National Lab. ORNL, O.R.T.U.: Amazon forest response to CO_2 fertilization dependent on
482   plant phosphorus acquisition. Nat. Geosci., 12, 736-741, doi: 10.1038/s41561-019-0404-9, 2019.

483 Gama-Rodrigues, A.C., Sales, M.V.S., Silva, P.S.D., Comerford, N.B., Cropper, W.P. and Gama-Rodrigues, E.F.: An
484   exploratory analysis of phosphorus transformations in tropical soils using structural equation modeling. Biogeochemistry,
485   118, 453-469, doi: 10.1007/s10533-013-9946-x, 2014.

486 Goll, D.S., Brovkin, V., Parida, B.R., Reick, C.H., Kattge, J., Reich, P.B., van Bodegom, P.M. and Niinemets, Ü.: Nutrient
487   limitation reduces land carbon uptake in simulations with a model of combined carbon, nitrogen and phosphorus cycling.
488   Biogeosciences, 9, 3547-3569, doi: 10.5194/bg-9-3547-2012, 2012.

489 Goll, D.S., Moosdorf, N., Hartmann, J. and Brovkin, V.: Climate-driven changes in chemical weathering and associated
490   phosphorus release since 1850: Implications for the land carbon balance. Geophys. Res. Lett., 41, 3553-3558, doi:
491   10.1002/2014GL059471, 2014.

492 Goll, D.S., Vuichard, N., Maignan, F., Jornet-Puig, A., Sardans, J., Violette, A., Peng, S., Sun, Y., Kvakic, M., Guimberteau,
493   M., Guenet, B., Zaehle, S., Penuelas, J., Janssens, I. and Ciais, P.: A representation of the phosphorus cycle for ORCHIDEE
494   (revision 4520). Geosci. Model Dev., 10, 3745-3770, doi: 10.5194/gmd-10-3745-2017, 2017.

495 Hahm, W.J., Riebe, C.S., Lukens, C.E. and Araki, S.: Bedrock composition regulates mountain ecosystems and landscape
496   evolution. Proceedings of the National Academy of Sciences, 111, 3338-3343, doi: 10.1073/pnas.1315667111, 2014.

497 He, X., Augusto L., Goll D.S., Ringeval B., Wang Y., Helfenstein J., Huang Y., Yu K., Wang Z., Yang Y. and Hou E.: Global
498   patterns and drivers of soil total phosphorus concentration, doi: 10.6084/m9.figshare.14583375, 2021.

499 Helfenstein, J., Tamburini, F., von Sperber, C., Massey, M.S., Pistocchi, C., Chadwick, O.A., Vitousek, P.M., Kretzschmar,
500   R. and Frossard, E.: Combining spectroscopic and isotopic techniques gives a dynamic view of phosphorus cycling in soil.
501   Nat. Commun., 9, doi: 10.1038/s41467-018-05731-2, 2018.

502 Hengl, T., Leenaars, J.G.B., Shepherd, K.D., Walsh, M.G., Heuvelink, G.B.M., Mamo, T., Tilahun, H., Berkhout, E., Cooper,
503   M., Fegraus, E., Wheeler, I. and Kwabena, N.A.: Soil nutrient maps of Sub-Saharan Africa: assessment of soil nutrient
504   content at 250 m spatial resolution using machine learning. Nutr. Cycl. Agroecosys., 109, 77-102, doi: 10.1007/s10705-
505   017-9870-x, 2017a.

506 Hengl, T., Mendes, D.J.J., Heuvelink, G.B., Ruiperez, G.M., Kilibarda, M., Blagotic, A., Shangguan, W., Wright, M.N., Geng,
507   X., Bauer-Marschallinger, B., Guevara, M.A., Vargas, R., MacMillan, R.A., Batjes, N.H., Leenaars, J.G., Ribeiro, E.,
508   Wheeler, I., Mantel, S. and Kempen, B.: SoilGrids250m: Global gridded soil information based on machine learning. PLoS
509   One, 12, e0169748, doi: 10.1371/journal.pone.0169748, 2017b.

510 Hou, E., Chen, C., Luo, Y., Zhou, G., Kuang, Y., Zhang, Y., Heenan, M., Lu, X. and Wen, D.: Effects of climate on soil
511   phosphorus cycle and availability in natural terrestrial ecosystems. Global Change Biol., 24, 3344-3356, doi:
512   10.1111/gcb.14093, 2018a.

513 Hou, E., Luo, Y., Kuang, Y., Chen, C., Lu, X., Jiang, L., Luo, X. and Wen, D.: Global meta-analysis shows pervasive
514   phosphorus limitation of aboveground plant production in natural terrestrial ecosystems. Nat. Commun., 11, 637, doi:

515   10.1038/s41467-020-14492-w, 2020.

516   Hou, E., Tan, X., Heenan, M. and Wen, D.: A global dataset of plant available and unavailable phosphorus in natural soils
517   derived by Hedley method. Scientific Data, 5, doi: 10.1038/sdata.2018.166, 2018b.

518   Hou, E., Wen, D., Jiang, L., Luo, X., Kuang, Y., Lu, X., Chen, C., Allen, K.T., He, X., Huang, X. and Luo, Y.: Latitudinal
519   patterns of terrestrial phosphorus limitation over the globe. Ecol. Lett., 00, 1-12, doi: 10.1111/ele.13761, 2021.

520   Huston, M.A.: Precipitation, soils, NPP, and biodiversity: resurrection of Albrecht's curve. Ecol. Monogr., 82, 277-296, doi:
521   10.1890/11-1927.1, 2012.

522   Huston, M.A. and Wolverton, S.: The global distribution of net primary production: resolving the paradox. Ecol. Monogr., 79,
523   343-377, doi: 10.1890/08-0588.1, 2009.

524   Jenny, H., Factors of soil formation; a system of quantitative pedology. McGraw-Hill, New York,1941.

525   Ji, H., Wen, J., Du, B., Sun, N., Berg, B. and Liu, C.: Comparison of the nutrient resorption stoichiometry of Quercus
526   variabilis Blume growing in two sites contrasting in soil phosphorus content. Ann. Forest Sci., 75, doi: 10.1007/s13595-
527   018-0727-5, 2018.

528   Kitayama, K., Majalap-Lee, N. and Aiba, S.: Soil Phosphorus Fractionation and Phosphorus-Use Efficiencies of Tropical
529   Rainforests along Altitudinal Gradients of Mount Kinabalu, Borneo. Oecologia, 123, 342-349, doi:
530   10.1007/s004420051020, 2000.

531   Kuhn, M.: caret: Classification and Regression Training. R package version 6.0-86., https://github.com/topepo/caret/, 2020.

532   Li, P., Yang, Y., Han, W. and Fang, J.: Global patterns of soil microbial nitrogen and phosphorus stoichiometry in forest
533   ecosystems. Global Ecol. Biogeogr., 23, 979-987, doi: 10.1111/geb.12190, 2014.

534   Li, X., Li, Y., Peng, S., Chen, Y. and Cao, Y.: Changes in soil phosphorus and its influencing factors following afforestation
535   in Northern China. Land Degrad. Dev., 30, 1655-1666, doi: 10.1002/ldr.3345, 2019.

536   Liaw, A. and Wiener, M.: Classification and Regression by randomForest. R News, 2, 18-22,2002.

537   Mage, S.M. and Porder, S.: Parent Material and Topography Determine Soil Phosphorus Status in the Luquillo Mountains of
538   Puerto Rico. Ecosystems, 16, 284-294, doi: 10.1007/s10021-012-9612-5, 2013.

539   McGroddy, M.E.: LBA-ECO TG-07 Forest Soil P, C, and N Pools, km 83 Site, Tapajos National Forest. Data set. Available
540   on-line [http://daac.ornl.gov] from Oak Ridge National Laboratory Distributed Active Archive Center, Oak Ridge,
541   Tennessee, U.S.A .http://dx.doi.org/10.3334/ORNLDAAC/1085.,2012.

542   Mehmood, A., Akhtar, M.S., Imran, M. and Rukh, S.: Soil apatite loss rate across different parent materials. Geoderma, 310,
543   218-229, doi: 10.1016/j.geoderma.2017.09.036, 2018.

544   Meinshausen, N.: Quantile Regression Forests. J. Mach. Learn. Res., 7, 983-999, doi: 10.5555/1248547.1248582, 2006.

545   Meinshausen, N.: quantregForest: Quantile Regression Forests, https://CRAN.R-project.org/package=quantregForest, 2017.

546   Minasny, B.M., Alex, B.M.M., Malone, P, B., B, A. and Budiman, Using R for Digital Soil Mapping. Springer, Cham, doi:
547   10.1007/978-3-319-44327-0, 2017.

548   Ploton, P., Mortier, F., Réjou-Méchain, M., Barbier, N., Picard, N., Rossi, V., Dormann, C., Cornu, G., Viennois, G., Bayol,
549   N., Lyapustin, A., Gourlet-Fleury, S. and Pélissier, R.: Spatial validation reveals poor predictive performance of large-
550   scale ecological mapping models. Nat. Commun., 11, 4540, doi: 10.1038/s41467-020-18321-y, 2020.

551   Porder, S. and Chadwick, O.A.: Climate and Soil-Age Constraints on Nutrient Uplift and Retention by Plants. Ecology, 90,
552   623-636, doi: 10.1890/07-1739.1, 2009.

553   Porder, S. and Ramachandran, S.: The phosphorus concentration of common rocks—a potential driver of ecosystem P status.
554   Plant Soil, 367, 41-55, doi: 10.1007/s11104-012-1490-2, 2013.

555   R Core Team: R: A language and environment for statistical computing. R Foundation for Statistical Computing, Vienna,
556   Austria, https://www.R-project.org/, 2018.

557   Reed, S.C., Yang, X. and Thornton, P.E.: Incorporating phosphorus cycling into global modeling efforts: a worthwhile,
558   tractable endeavor. New Phytologist, 208, 324-329, doi: 10.1111/nph.13521, 2015.

559   Reich, P.B. and Oleksyn, J.: Global patterns of plant leaf N and P in relation to temperature and latitude. Proceedings of the
560   National Academy of Sciences, 101, 11001-11006, doi: 10.1073/pnas.0403588101, 2004.

561   Ringeval, B., Augusto, L., Monod, H., van Apeldoorn, D., Bouwman, L., Yang, X., Achat, D.L., Chini, L.P., Van Oost, K.,

562   Guenet, B., Wang, R., Decharme, B., Nesme, T. and Pellerin, S.: Phosphorus in agricultural soils: drivers of its distribution
563   at the global scale. Global Change Biol., 23, 3418-3432, doi: 10.1111/gcb.13618, 2017.

564   Rodionov, A., Bauke, S.L., von Sperber, C., Hoeschen, C., Kandeler, E., Kruse, J., Lewandowski, H., Marhan, S., Mueller,
565   C.W., Simon, M., Tamburini, F., Uhlig, D., von Blanckenburg, F., Lang, F. and Amelung, W.: Biogeochemical cycling of
566   phosphorus in subsoils of temperate forest ecosystems. Biogeochemistry, 150, 313-328, doi: 10.1007/s10533-020-00700-
567   8, 2020.

568   Shangguan, W., Dai, Y., Duan, Q., Liu, B. and Yuan, H.: A global soil data set for earth system modeling. J. Adv. Model.
569   Earth Sy., 6, 249-263, doi: 10.1002/2013MS000293, 2014.

570   Shangguan, W., Hengl, T., Mendes De Jesus, J., Yuan, H. and Dai, Y.: Mapping the global depth to bedrock for land surface
571   modeling. J. Adv. Model. Earth Sy., 9, 65-88, doi: 10.1002/2016MS000686, 2017.

572   Siqueira, R.G., Schaefer, C.E.G.R., Fernandes Filho, E.I., Corrêa, G.R., Francelino, M.R., Souza, J.J.L.L. and Rocha, P.D.A.:
573   Weathering and pedogenesis of sediments and basaltic rocks on Vega Island, Antarctic Peninsula. Geoderma, 382, 114707,
574   doi: 10.1016/j.geoderma.2020.114707, 2021.

575   Smeck, N.E.: Phosphorus dynamics in soils and landscapes. Geoderma, 36, 185-199, doi: 10.1016/0016-7061(85)90001-1,
576   1985.

577   Smil, V.: Phosphorus in the environment: natural flows and human interferences. Annual Review of Energy and the
578   Environment, 25, 53-88, doi: 10.1146/annurev.energy.25.1.53, 2000.

579   Spohn, M.: Increasing the organic carbon stocks in mineral soils sequesters large amounts of phosphorus. Global Change Biol.,
580   26, 4169-4177, doi: 10.1111/gcb.15154, 2020.

581   Strobl, C., Boulesteix, A., Kneib, T., Augustin, T. and Zeileis, A.: Conditional variable importance for random forests. BMC
582   Bioinformatics, 9, 307, doi: 10.1186/1471-2105-9-307, 2008.

583   Sun, Y., Peng, S., Goll, D.S., Ciais, P., Guenet, B., Guimberteau, M., Hinsinger, P., Janssens, I.A., Peñuelas, J., Piao, S.,
584   Poulter, B., Violette, A., Yang, X., Yin, Y. and Zeng, H.: Diagnosing phosphorus limitations in natural terrestrial
585   ecosystems in carbon cycle models. Earth's Future, 5, 730-749, doi: 10.1002/2016EF000472, 2017.

586   Tipping, E., Somerville, C.J. and Luster, J.: The C:N:P:S stoichiometry of soil organic matter. Biogeochemistry, 130, 117-131,
587   doi: 10.1007/s10533-016-0247-z, 2016.

588   Turner, B.L. and Engelbrecht, B.M.J.: Soil organic phosphorus in lowland tropical rain forests. Biogeochemistry, 103, 297-
589   315, doi: 10.1007/s10533-010-9466-x, 2011.

590   Viscarra Rossel, R.A. and Bui, E.N.: A new detailed map of total phosphorus stocks in Australian soil. Sci. Total Environ.,
591   542, 1040-1049, doi: 10.1016/j.scitotenv.2015.09.119, 2016.

592   Vitousek, P.M. and Chadwick, O.A.: Pedogenic Thresholds and Soil Process Domains in Basalt-Derived Soils. Ecosystems,
593   16, 1379-1395, doi: 10.1007/s10021-013-9690-z, 2013.

594   Vitousek, P.M., Porder, S., Houlton, B.Z. and Chadwick, O.A.: Terrestrial phosphorus limitation: mechanisms, implications,
595   and nitrogen–phosphorus interactions. Ecol. Appl., 20, 5-15, doi: 10.1890/08-0127.1, 2010.

596   Walker, T.W. and Syers, J.K.: The fate of phosphorus during pedogenesis. Geoderma, 15, 1-19, doi: 10.1016/0016-
597   7061(76)90066-5, 1976.

598   Wang, Y., Law, R.M. and Pak, B.: A global model of carbon, nitrogen and phosphorus cycles for the terrestrial biosphere.
599   Biogeosciences, 7, 2261-2282, doi: 10.5194/bg-7-2261-2010, 2010.

600   Wang, Y., Zhang, Q., Pitman, A.J. and Dai, Y.: Nitrogen and phosphorous limitation reduces the effects of land use change
601   on land carbon uptake or emission. Environ. Res. Lett., 10, 14001, doi: 10.1088/1748-9326/10/1/014001, 2015.

602   Wang, Y., Zhang, X. and Huang, C.: Spatial variability of soil total nitrogen and soil total phosphorus under different land
603   uses in a small watershed on the Loess Plateau, China. Geoderma, 150, 141-149, doi: 10.1016/j.geoderma.2009.01.021,
604   2009.

605   Wang, Z., Tian, H., Yang, J., Shi, H., Pan, S., Yao, Y., Banger, K. and Yang, Q.: Coupling of Phosphorus Processes With
606   Carbon and Nitrogen Cycles in the Dynamic Land Ecosystem Model: Model Structure, Parameterization, and Evaluation
607   in Tropical Forests. J. Adv. Model. Earth Sy., 12, e2020MS002123, doi: 10.1029/2020MS002123, 2020.

608   Wang, Z., Wang, M., Yu, K., Hu, H., Yang, Y., Ciais, P., Ballantyne, A.P., Niklas, K.J., Huang, H., Yao, B. and Wright, S.J.:

609   Global synthesis for the scaling of soil microbial nitrogen to phosphorus in terrestrial ecosystems. Environ. Res. Lett., 16,
610   044034, doi: 10.1088/1748-9326/abed78, 2021.

611   Wardle, D.A., Walker, L.R., Bardgett, R.D. and Sveriges, L.: Ecosystem Properties and Forest Decline in Contrasting Long-
612   Term Chronosequences. Science, 305, 509-513, doi: 10.1126/science.1098778, 2004.

613   Wassen, M.J., Schrader, J., van Dijk, J. and Eppinga, M.B.: Phosphorus fertilization is eradicating the niche of northern
614   Eurasia's threatened plant species. Nature Ecology & Evolution, 5, 67-73, doi: 10.1038/s41559-020-01323-w, 2021.

615   Wieder, W.R., Cleveland, C.C., Smith, W.K. and Todd-Brown, K.: Future productivity and carbon storage limited by terrestrial
616   nutrient availability. Nat. Geosci., 8, 441-444, doi: 10.1038/ngeo2413, 2015.

617   Xu, X., Thornton, P.E. and Post, W.M.: A global analysis of soil microbial biomass carbon, nitrogen and phosphorus in
618   terrestrial ecosystems. Global Ecol. Biogeogr., 22, 737-749, doi: 10.1111/geb.12029, 2013.

619   Yan, T., Zhu, J. and Yang, K.: Leaf nitrogen and phosphorus resorption of woody species in response to climatic conditions
620   and soil nutrients: a meta-analysis. Journal of forestry research, 29, 905-913, doi: 10.1007/s11676-017-0519-z, 2018.

621   Yanai, R.D.: The effect of whole-tree harvest on phosphorus cycling in a northern hardwood forest. Forest Ecol. Manag., 104,
622   281-295, doi: 10.1016/S0378-1127(97)00256-9, 1998.

623   Yang, X., Post, W.M., Thornton, P.E. and Jain, A.: The distribution of soil phosphorus for global biogeochemical modeling.
624   Biogeosciences, 10, 2525-2537, doi: 10.5194/bg-10-2525-2013, 2013.

625   Yang, X., Thornton, P.E., Ricciuto, D.M. and Post, W.M.: The role of phosphorus dynamics in tropical forests - a modeling
626   study using CLM-CNP. Biogeosciences, 11, 1667-1681, doi: 10.5194/bg-11-1667-2014, 2014.

627   Zhang, C., Tian, H., Liu, J., Wang, S., Liu, M., Pan, S. and Shi, X.: Pools and distributions of soil phosphorus in China. Global
628   Biogeochem. Cy., 19, GB1020, doi: 10.1029/2004GB002296, 2005.

629   Zhang, Q., Wang, Y.P., Pitman, A.J. and Dai, Y.J.: Limitations of nitrogen and phosphorous on the terrestrial carbon uptake
630   in the 20th century. Geophys. Res. Lett., 38, L22701, doi: 10.1029/2011GL049244, 2011.

631   Zhang, Y., Guo, Y., Tang, Z., Feng, Y., Zhu, X., Xu, W., Bai, Y., Zhou, G., Xie, Z. and Fang, J.: Patterns of nitrogen and
632   phosphorus pools in terrestrial ecosystems in China [preprint]. Earth Syst. Sci. Data Discuss, doi: 10.5194/essd-2020-398,
633   2021.

634

635

636